Modeling the effects of cyclodextrin on intracellular membrane vesicles from Cos-7 cells prepared by sonication and carbonate treatment

Peter Kilbride, Holly J. Woodward, Kuan Boone Tan, Nguyễn T.K. Thanh, K.M. Emily Chu, Shane Minogue, Mark G Waugh

Cholesterol has important functions in the organization of membrane structure and this may be mediated via the formation of cholesterol-rich, liquid-ordered membrane microdomains often referred to as lipid rafts. Methyl-beta-cyclodextrin (cyclodextrin) is commonly used in cell biology studies to extract cholesterol and therefore disrupt lipid rafts. However, in this study we reassessed this experimental strategy and investigated the effects of cyclodextrin on the physical properties of sonicated and carbonate-treated intracellular membrane vesicles isolated from Cos-7 fibroblasts. We treated these membranes, which mainly originate from the *trans*-Golgi network and endosomes, with cyclodextrin and measured the effects on their equilibrium buoyant density, protein content, represented by the palmitoylated protein phosphatidylinositol 4-kinase type IIalpha, and cholesterol. Despite the reduction in mass stemming from cholesterol removal, the vesicles became denser, indicating a possible large volumetric decrease, and this was confirmed by measurements of hydrodynamic vesicle size. Subsequent mathematical analyses demonstrated that only half of this change in membrane size was attributable to cholesterol loss. Hence, the non-selective desorption properties of cyclodextrin are also involved in membrane size and density changes. These findings may have implications for preceding studies that interpreted cyclodextrin-induced changes to membrane biochemistry in the context of lipid raft disruption without taking into account our finding that cyclodextrin treatment also reduces membrane size.

Modeling the effects of cyclodextrin on intracellular membrane vesicles from Cos-7 cells prepared by sonication and carbonate treatment

Authors: Peter Kilbride*, Holly J. Woodward*, Kuan B. Tan[#$], Nguyễn T. K. Thanh[#], K.M. Emily Chu*, Shane Minogue* and Mark G. Waugh*[$]

Address *UCL Institute for Liver & Digestive Health
Royal Free Campus,
University College London
Rowland Hill Street
London NW3 2PF
United Kingdom

[#] Biophysics Group
Department of Physics & Astronomy
University College London
Gower Street,
London WC1E 6BT
United Kingdom &
UCL Healthcare Biomagnetic and Nanomaterials Laboratories
21 Albemarle Street,
London W1S 4BS
United Kingdom

[$] **Corresponding author; e-mail:** m.waugh@ucl.ac.uk

Running Title: Membrane size and cholesterol

Abbreviations: Cyclodextrin – methyl-β-cyclodextrin, DMEM – Dulbecco's Modified Eagle's Medium, ECL – enhanced chemiluminescence, HRP – horseradish peroxidase, PBS – phosphate-buffered saline, OCRL – oculocerebrorenal syndrome of Lowe, PI4KIIα – phosphatidylinositol 4-kinase type IIα, PVDF – polyvinylidene difluoride, SDS-PAGE – sodium dodecyl sulfate-polyacrylamide gel electrophoresis, TGN – *trans*-Golgi network.

Keywords: Cholesterol; cyclodextrin; lipid raft; membrane; TGN, PI 4-kinase.

Abstract

Cholesterol has important functions in the organization of membrane structure and this may be mediated via the formation of cholesterol-rich, liquid-ordered membrane microdomains often referred to as lipid rafts. Methyl-β-cyclodextrin (cyclodextrin) is commonly used in cell biology studies to extract cholesterol and therefore disrupt lipid rafts. However, in this study we reassessed this experimental strategy and investigated the effects of cyclodextrin on the physical properties of sonicated and carbonate-treated intracellular membrane vesicles isolated from Cos-7 fibroblasts. We treated these membranes, which mainly originate from the *trans*-Golgi network and endosomes, with cyclodextrin and measured the effects on their equilibrium buoyant density, protein content, represented by the palmitoylated protein phosphatidylinositol 4-kinase type IIα, and cholesterol. Despite the reduction in mass stemming from cholesterol removal, the vesicles became denser, indicating a possible large volumetric decrease, and this was confirmed by measurements of hydrodynamic vesicle size. Subsequent mathematical analyses demonstrated that only half of this change in membrane size was attributable to cholesterol loss. Hence, the non-selective desorption properties of cyclodextrin are also involved in membrane size and density changes. These findings may have implications for preceding studies that interpreted cyclodextrin-induced changes to membrane biochemistry in the context of lipid raft disruption without taking into account our finding that cyclodextrin treatment also reduces membrane size.

Introduction

In this study we investigated the relationship between membrane composition, density, and size by using methyl-β-cyclodextrin (cyclodextrin) to rapidly deplete membrane cholesterol from an isolated intracellular membrane preparation. Cyclodextrins are a family of cyclic oligosaccharides that adopt a cone-like structure in aqueous solution, with an internal hydrophobic core that can sequester lipids from membranes (Heine et al., 2007; Pinjari et al., 2006). Cyclodextrins have useful pharmaceutical applications as soluble carriers for hydrophobic molecules and are also commonly used in biochemical and cell biology studies to manipulate membrane lipid levels (Loftsson and Brewster, 1996; Rodal et al., 1999; Welliver, 2006; Zidovetzki and Levitan, 2007). Cyclodextrin efficaciously removes sterols such as cholesterol from biological membranes but can also release other lipids such as sphingomyelin and phosphatidylcholine (Ottico et al., 2003). Recently cyclodextrin and the related molecule hydroxypropyl-β-cyclodextrin have been shown to alleviate the pathological intracellular accumulation of free cholesterol in Niemann-Pick Type C disease models (Camargo et al., 2001; Davidson et al., 2009; Holtta-Vuori et al., 2002; Lim et al., 2006; Liu et al., 2008; Liu et al., 2010; Liu et al., 2009; Mbua et al., 2013; Pontikis et al., 2013; Ramirez et al.; Ramirez et al., 2010; Rosenbaum et al., 2010; Swaroop et al., 2012; te Vruchte et al., 2014; Vance and Karten, 2014; Vite et al., 2015; Waugh, 2015). These recent developments demonstrate a potential therapeutic use for cyclodextrins and also clearly establish their efficacy for reducing the cholesterol content of endosomal membranes (Rosenbaum et al., 2010; Shogomori and Futerman, 2001). In addition, we have previously reported that the addition of cyclodextrin to cultured cells leads to the vesicularization and contraction of the *trans*-Golgi network (TGN) and endosomal membranes (Minogue et al., 2010). These cyclodextrin-induced changes to

intracellular biomembrane architecture are associated with alterations to intramembrane lateral diffusion and lipid kinase activity of phosphatidylinositol 4-kinase IIα (PI4KIIα), a constitutively palmitoylated and membrane-associated enzyme (Barylko et al., 2009; Lu et al., 2012) that may be important in the etiology of some cancers and neurodegenerative disorders (Chu et al., 2010; Clayton et al., 2013a; Li et al., 2010; Li et al., 2014; Simons et al., 2009; Waugh, 2012, 2014, 2015).

Whilst cyclodextrin has been mainly used to remove cholesterol from the plasma membrane our focus here is on characterizing the effects of such treatment on intracellular membranes where cholesterol levels are known to be important for processes such as protein sorting and trafficking from the TGN (Paladino et al., 2014). Since the effects of cyclodextrin on intracellular membranes are important to understand both in a disease context (Vite et al., 2015) and for furthering our knowledge about the functions of cholesterol on intracellular membranes, we decided to investigate more comprehensively how cyclodextrin alters the biophysical properties of a lipid-raft-enriched membrane fraction isolated from intracellular TGN and endosomal membranes (Minogue et al., 2010; Waugh et al., 2011a). In particular, we sought to understand more fully the cyclodextrin-induced changes to the equilibrium buoyant densities of isolated cholesterol-rich membrane fractions that we and others have reported in a number of preceding publications (for examples, see (Hill et al., 2002; Kabouridis et al., 2000; Matarazzo et al., 2012; Minogue et al., 2010; Navratil et al., 2003; Pike and Miller, 1998; Spisni et al., 2001; Xu et al., 2006; Zidovetzki and Levitan, 2007)). In these previous experiments, cholesterol depletion with cyclodextrin rendered the membrane fraction less buoyant, leading to the cyclodextrin-treated membranes banding to a denser region in an equilibrium density gradient. This cyclodextrin-induced change, sometimes referred to as a density shift, has

allowed us to design, using sucrose density gradients, a membrane floatation assay in which we have been able to separate cholesterol-replete and -depleted membranes before and after cyclodextrin treatment.

In many of these prior studies, a cyclodextrin-dependent redistribution of biomolecules to a denser membrane fraction was interpreted as a delocalization from cholesterol-rich lipid rafts or liquid-ordered domains to a less buoyant, liquid-disordered, non-raft fraction. This reasoning stems from the idea that raft-enriched membrane domains are intrinsically buoyant due to their high lipid-to-protein ratio. However, since density is defined as mass divided by volume we reassessed these inferences on the grounds that in the absence of a membrane volume change, a reduction in mass alone would result in a membrane becoming more buoyant, i.e. less dense.

To explore the relationship between cholesterol content and membrane density, we employed our membrane floatation assay to measure the change in the physical properties and biochemical composition of cholesterol-enriched membrane vesicles following cyclodextrin treatment. We then analyzed these changes to mathematically model, from first principles, the degree to which the mass and volume of the membrane domains would have to alter in order to account for the measured change in membrane density. Finally, we provide a mathematical solution to explain the relationship between membrane cholesterol mass and vesicle density.

Materials and Methods

Materials. All cell culture materials, enhanced chemiluminescence (ECL) reagents and X-ray film were purchased from GE Healthcare Life Sciences, UK. Polyvinylidene difluoride (PVDF) membrane was bought from Merck Millipore UK. Horseradish peroxidase (HRP)-linked

secondary antibodies were purchased from Cell Signalling Technology UK. The antibody to PI4KIIα was previously described by us (Minogue et al., 2010). HRP-linked cholera toxin B subunit was purchased from Sigma-Aldrich UK. Sucrose was obtained from VWR International Ltd UK. Complete protease inhibitor tablets were purchased from Roche Ltd UK. All other reagents were from Sigma-Aldrich UK

Cell culture. Cos-7 cells obtained from the European Collection of Cell Cultures operated by Public Health England were maintained at 37°C in a humidified incubator at 10% CO_2. Cells were cultured in Dulbecco's Modified Eagle's Medium (DMEM) supplemented with Glutamax, 10% fetal calf serum, 50 i.u./mL penicillin, and 50 μg/mL streptomycin. Cell monolayers were grown to confluency in 10 cm tissue culture dishes. Typically, four confluent plates of cells were used in each subcellular fractionation experiment.

Subcellular fractionation by sucrose density gradient centrifugation. A buoyant subcellular fraction enriched for TGN and endosomal membranes was prepared according to our previously published method (Minogue et al., 2010; Waugh et al., 2006). Confluent cell monolayers were washed twice in ice-cold phosphate-buffered saline (PBS) pH 7.4 and then scraped into 2 mL of homogenization buffer (Tris-HCl 10mM, EGTA 1 mM, EDTA 1 mM, sucrose 250 mM, plus Complete™ protease inhibitors, pH 7.4). Post-nuclear supernatants were prepared by Dounce homogenization of the cells suspended in homogenization buffer followed by centrifugation at 1,000 *g* at 4°C for 2 min to pellet nuclei and unbroken cells. Cellular organelles were separated by equilibrium density gradient centrifugation by overnight ultracentrifugation on a 12 mL, 10–40% w/v sucrose density gradient as previously described (Waugh et al., 2003a; Waugh et al., 2003b; Waugh et al., 2006). Using this procedure, a buoyant

TGN-endosomal enriched membrane fraction consistently banded in gradient fractions 9 and 10 and was harvested as described before (Waugh et al., 2003b; Waugh et al., 2006).

Refractometry to measure membrane density. The refractive index of each membrane fraction was determined using a Leica AR200 digital refractometer. Refractive index values were then converted to sucrose densities using Blix tables (Dawson et al., 1986) and linear regression carried out using GraphPad Prism software.

Membrane floatation assay to measure the equilibrium buoyant density of membrane vesicles. This assay was previously described by us (Minogue et al., 2010). Briefly, 400 μL of cyclodextrin (20 mM) dissolved in water was added to an equal volume of TGN/endosomal membranes on ice for 10 min to give a cyclodextrin concentration of 10 mM. Then, 200 μL of sodium carbonate (0.5 M, pH 11.0) was added to a final concentration of 50 mM in a 1 mL sample. The carbonate-treated membranes were probe-sonicated on ice using a VibraCell probe sonicator from Sonics & Materials Inc, USA at amplitude setting 40 in pulsed mode for 3 x 2 sec bursts. To the 1 mL sonicated membrane samples, 3 mL of 53% w/v sucrose in Tris-HCl 10 mM, EDTA 1 mM and EGTA 1 mM, pH 7.4 was added to form 4 mL of sample in 40% w/v sucrose and a sodium carbonate concentration of 12.5 mM and, where applicable, a cyclodextrin concentration of 2 mM. A discontinuous sucrose gradient was formed in a 12 mL polycarbonate tube by overlaying the 40% sucrose layer with 4 mL 35% w/v and 4 mL 5% w/v sucrose in Tris-HCl 10 mM, EDTA 1 mM and EGTA 1 mM, pH 7.4. The gradient was centrifuged overnight at 185,000 *g* at 4°C in a Beckman LE-80K ultracentrifuge and 12 x 1 mL fractions were harvested beginning at the top of the tube.

Immunoblotting of sucrose density gradient fractions. The protein content of equal volume aliquots of each density gradient fraction was separated by sodium dodecyl sulfate-

polyacrylamide gel electrophoresis (SDS-PAGE), transferred to PVDF membranes and probed with antibodies directed against proteins of interest. Western blots were visualized by chemiluminescence and bands were quantified from scanned X-ray films using image analysis software in Adobe Photoshop CS4.

Measurements of membrane lipid levels. The cholesterol content of equal volume membrane fractions was assayed using the Amplex red cholesterol assay kit (Molecular Probes). The use of this assay to measure membrane cholesterol mass has been previously validated (Bate et al., 2008; Minogue et al., 2010; Nicholson and Ferreira, 2009). Ganglioside glycosphingolipids were detected by dot blotting of membrane fractions (Ilangumaran et al., 1996) and probing with HRP-conjugated cholera toxin B subunit as described previously (Ilangumaran et al., 1996; Mazzone et al., 2006; Waugh, 2013; Waugh et al., 2011a; Waugh et al., 2011b). Membrane-bound cholera toxin was visualized by incubation with chemiluminescence detection reagents and spots were quantified as described for the analysis of immunoblotting data (Waugh, 2013).

Dynamic light scattering measurement to measure hydrodynamic diameter of membrane vesicles. The hydrodynamic size of the membrane vesicles in the gradient fraction was studied with a Zetasizer Nano ZS90 (Malvern Instruments). All diluted samples were prepared in filtered (0.2 µm) Millipore ddH_2O to avoid sample artifacts, and measurements were made at 25°C in triplicate.

Mathematical modelling of membrane compositional changes.

Nomenclature

ρ = mass density (kg/L)

187 V = volume (L)

188 Subscripts are used to specify a unit being examined, with s and r defining treatment sensitive
189 (assuming that most of this fraction is composed of cholesterol with a density of around ρ =
190 1.067) and remaining components, respectively. The subscript –post is used to denote values
191 for vesicles post cyclodextrin treatment.

192 The fractions are not considered discrete sections of the vesicles; rather they can be mixed and
193 inter-connected.

194 The mass density of a particle is defined as the mass per unit volume. To determine the mass
195 density of an object consisting of multiple discrete components in a steady state, a linear
196 combination of its components can be used as in equation [1].

197

198 $$\rho = \frac{m_1 + m_2 + m_3 + \ldots}{V_1 + V_2 + V_3 + \ldots}$$

199 **[1]**

200

201 where the subscripts denote the mass and volume of the separate components. Through
202 normalizing the total volume V=V_1+V_2+V_3+…=1, the density can simplify to $\rho = m_1 + m_2 + m_3$
203 $+ \ldots m_n$

where m_n now refers to the mass of the volume fraction in question. Considering an object composed of n different materials the overall mass density is therefore

$$\rho_{whole} = \rho_{fraction1}V_{fraction1} + \rho_{fraction2}V_{fraction2} + \rho_{fraction3}V_{fraction3} + \ldots$$
$$= \sum_{j=1}^{j=n} \rho_j V_j$$

[2]

where ρ_j is the density of fraction j, and v_j is the volume fraction of material j.

To determine the % composition of the vesicles, boundary conditions were formulated and solved using simultaneous equations. Pre-treatment, the system was described through Equation [3]:

$$V_r \times \rho_r + V_s \times \rho_s = \rho_{pre}$$

[3]

where the fractional volume of the residual component is given by V_r, the fractional volume of the treatment sensitive component = V_s, and ρ_{pre} was the measured density of the vesicle pre-treatment.

A second simultaneous equation arises through the physical definition of the system, which is the total volume has been normalised to one:

$$V_r + V_s = 1$$

[4]

i.e. combining all the fractions in a vesicle together equaled fraction one of a vesicle.

The 3rd simultaneous equation was determined with respect to the post-treatment density. It can be derived that for the cyclodextrin sensitive fraction:

$$\rho_{pre} = \frac{m_{pre}}{V_{pre}} = \rho_{post} = \frac{m_{post}}{V_{post}} = 1.067$$

[5]

While the mass and volume of the cholesterol fraction change, its intrinsic density does not. Hence:

$$\frac{m_{pre}}{V_{pre}} = \frac{m_{post}}{V_{post}} \Rightarrow V_{post} = \frac{m_{post}}{m_{pre}} \times V_{pre}$$

[6]

233

234 $\frac{m_{post}}{m_{pre}}$ = the mass post-treatment relative to the pre-treatment mass, which was defined as the

235 dimensionless parameter M. The RHS of Equation [6] then simplified to: $V_{s\text{-}pre}$ x M. A similar

236 procedure was followed for V_r.

237 In order to define the mass density of the vesicles post-treatment, equation [3] was modified

238 and normalized to take account of the change of mass. This yielded:

239 $$\rho_{post} = \frac{V_r \times \rho_r + V_s \times \rho_s \times M_{s-post}}{V_r + V_s \times M_{s-post}}$$

240 **[7]**

241

242 **Statistical analysis.** Data are presented as mean ± SEM of at least three determinations.

243 Statistical significance was assessed using the two-tailed student t test and P values < 0.05 were

244 deemed to be statistically significant.

245

246 **Results**

247 **Changes in membrane composition and density following cholesterol depletion.** The starting

248 material for this set of experiments was our previously characterized cholesterol-rich

249 intracellular membrane fraction prepared from post-nuclear cell supernatants. These

membranes were isolated on equilibrium sucrose density gradients and their identity as a TGN-endosomal fraction was confirmed by Western blotting for PI4KIIα and syntaxin-6 (Minogue et al., 2010; Waugh et al., 2006). To investigate in more detail the relationship between cholesterol levels, membrane composition and membrane biophysical properties, we employed our recently described floatation assay method to determine the equilibrium buoyant densities of TGN-endosomal membrane domains using sucrose gradients (see work flow chart in Figure 1). This technique involved treating the membranes with cyclodextrin (10 mM) for 10 min to extract cholesterol followed by probe sonication to induce their vesicularization and fragmentation (Waugh et al., 1999; Waugh et al., 1998). The sonication step was carried out in alkaline carbonate buffer which is a well-established means for removing peripheral proteins including actin from membranes (Fujiki et al., 1982; Nebl et al., 2002). This procedure was necessary in light of the extensive literature demonstrating that peripherally associated membrane proteins can influence membrane architecture, geometry and density, and such additional heterogeneity in these membrane characteristics could potentially complicate subsequent biophysical analyses. This combination of probe sonication and carbonate addition was aimed at generating a population of membrane vesicles stripped of peripheral proteins including cyclodextrin-sensitive cytoskeletal proteins which have the potential to modify membrane microdomain stability [46-49]. Furthermore, the inclusion of these treatments meant that the integral protein and lipid compositions of the vesicles would be the principal determinants of membrane density.

In this set of experiments we compared the effects of cyclodextrin treatment on the biochemical composition of the buoyant (fractions 5 to 8) and dense (fractions 9 to 12) regions of the sucrose gradient. Cyclodextrin addition resulted in a large (83.4 ± 2.75%, n = 3) decrease

in the cholesterol mass of the buoyant fractions protein without any significant accumulation in the denser region of the sucrose gradient (Figure 2). This large reduction in cholesterol also coincided with a relocalization of the membrane-associated PI4KIIα protein to denser membrane fractions 9 to 12 (Figure 2). We quantified this change in PI4KIIα distribution, which was also noted in our previous publication (Minogue et al., 2010), and found that unlike the situation with cholesterol, cyclodextrin did not result in an overall loss of PI4KIIα from the membrane fractions.

We used refractometry to measure the sucrose density of the gradient fractions. Trial experiments revealed that the final, diluted cyclodextrin concentrations of 200 mM present in the dense gradient fractions did not impact on the refractive index readings for these samples. These measurements allowed us to determine that the inclusion of cyclodextrin caused the main protein fraction to shift in density from 1.096 to 1.126 g/mL (Figure 3).

Finally, we measured cyclodextrin-effected changes to the hydrodynamic diameter of the vesicles by dynamic light scattering. Even though the isolated membrane vesicles were found to be heterogeneous we focused on a peak signal corresponding to a vesicle population in the biologically relevant size range of 10-1000 nm. We ascertained that while there was no change in the total number of vesicles, the average vesicle diameter shrunk from 780 to 42 nm in the buoyant fraction and from 453 to 271 nm in the dense fraction (Table 1). These results showed that the reduction in cholesterol levels brought about by cyclodextrin treatment caused the membrane vesicle sizes to decrease considerably.

Together, these experiments revealed that cholesterol depletion with cyclodextrin resulted in a reduction in membrane buoyancy, as evidenced by the delocalization of PI4KIIα-containing membranes to a denser region of the sucrose gradient and also a reduction in membrane size.

296 Therefore, we decided to mathematically model the relationship between these different
297 parameters.

298

299 **Mathematical Modeling**

300 In this model, we determined an expected value for vesicle size post cyclodextrin treatment in
301 our system and compared it with experimental data. From our experimental measurements,
302 there was an 83.4 ± 2.75%, reduction in the cyclodextrin sensitive cholesterol component with
303 other components not directly affected by the treatment. The total increase in mass density of
304 the vesicles through cyclodextrin treatment was known (from 1.096 ± 0.003 mg/mL for fraction
305 5 to 1.122 ± 0.0005 mg/mL for fraction 10). The % composition of these two components and
306 the density of the non-cholesterol residual component were unknown and approximated in this
307 work, based on the above assumptions.

308 To determine the volumetric fractional composition of the vesicles pre cyclodextrin treatment
309 and the density of the residual component, the experimentally measured values were inserted
310 into equations 4,6, and 7, giving equations 8-10:

311

312 $$V_r \times \rho_r + V_s \times 1.067 = 1.096 \pm 0.003$$

313 **[8]**

314 $$V_r + V_s = 1$$

315 **[9]**

316 $$\frac{V_r \times \rho_r + V_s \times 1.067 \times (0.166 \pm 0.00275)}{V_r + V_s \times (0.166 \pm 0.00275)} = 1.122 \pm 0.0005$$

317 **[10]**

318

319 Calculating these equations [8] to [10] allowed us to predict the volume fractions of the vesicle
320 pretreatment as follows – cholesterol 0.567 ± 0.072 (56.7 ± 7.2%), residual component 0.433 ±
321 0.072 (43.3 ± 7.2%), and a density of the residual component of 1.134 ± 0.005 mg/mL. As liquid-
322 ordered domains typically comprises 20–30% cholesterol, the higher than expected value
323 determined here is most likely the result of some membrane components being removed
324 during the membrane isolation procedure and particularly by the alkaline carbonate addition
325 step, leading to an apparent enrichment of cholesterol in the isolated fraction. Hence, the %
326 value for cholesterol determined here is not the physiological proportion of cholesterol in
327 TGN/endosomal membranes but rather, the amount present in the membrane vesicles after
328 the extensive membrane disruption and isolation procedures used in this study. In concordance
329 with this explanation, we have previously shown that membrane fractions prepared in the
330 presence of carbonate are subject to substantial depletion of non-integral proteins (Waugh,
331 2013; Waugh et al., 2011a; Waugh et al., 2011b). As proteins have a density of 1.35 mg/mL
332 (Chick and Martin, 1913; Fischer et al., 2004) and other membrane components such as lipids
333 tend to have much lower densities, the value of 1.134 ± 0.005 mg/mL calculated for the density
334 of the residual component seems reasonable.

335 Cyclodextrin treatment resulted in the total amount of cholesterol in the system to be reduced
336 by 83.4%; however, the absolute volumes of the other components remained constant. To

337 calculate the volume concentrations post cyclodextrin, three more simultaneous equations
338 were formulated and solved by the same method:

339

340 $$V_{r-post} \times \rho_r + V_{s-post} \times 1.067 = 1.122 \pm 0.0005$$

341 **[11]**

342 $$V_{r-post} + V_{s-post} = 1$$

343 **[12]**

344 $$\frac{V_{r-post} \times \rho_r + V_{s-post} \times 1.067 \times 6.02}{V_{r-post} + V_{s-post} \times 6.02} = 1.096 \pm 0.03$$

345 **[13]**

346 The predicted vesicle composition post treatment obtained by solving any two of equations [11]
347 to [13] was: cholesterol 0.179 ± 0.047 (17.9 ± 4.7%) and residual component 0.821 ± 0.047 (82.1
348 ± 4.7%).

349

350 The relative volume of the treated vesicles was calculated through equation [14]:

351

352

353 $$V_r + V_s \times 0.166 \pm 0.0275 = New\ Volume$$

354 **[14]**

355 giving a relative volume of 0.527 ± 0.073, i.e. post treatment, the vesicle was 49.1 ± 7.3% of its
356 original size. This corresponds to the diameter of the treated vesicles of 0.81 ± 0.04, i.e. the
357 radius must have shrunk by 19 ± 4%.

358

359 Experimental measurements showed the diameter of the vesicles falling from 453 ± 177.1 nm
360 to 270.2 ± 68.8 nm post treatment, a 40.4% decline in diameter and thus an 88.8% fall in vesicle
361 volume. This differs markedly from what has been calculated based on cyclodextrin affecting
362 cholesterol alone and is consistent with previous work demonstrating that cyclodextrin can also
363 sequester a range of hydrophobic molecules (reviewed in (Zidovetzki and Levitan, 2007)). These
364 results imply that only about 50% of the change in membrane size is due to cholesterol
365 desorption.

366 Since the mathematical analysis demonstrated that the decrease in membrane size could not
367 be fully accounted for by cholesterol loss, we investigated the effect of cyclodextrin addition on
368 the levels of membrane gangliosides which are glycosphingolipids that are structurally
369 unrelated to sterols. Changes in ganglioside lipid distribution were determined using HRP-
370 conjugated cholera toxin B subunit as a probe. Kuziemko and colleagues (Kuziemko et al.,
371 1996) previously determined that Cholera-toxin binds to gangliosides in the order GM1 > GM2
372 > GD1A > GM3 > GT1B > GD1B > asialo-GM1, albeit with a > 200 fold difference in binding
373 affinity between GM1 and asialo-GM1. Unlike thin layer chromatography, dot-blotting
374 immobilized sucrose density gradient fractions with cholera toxin B subunit do not permit the
375 separation and quantitation of individual glycosphingolipid species. However we used this well
376 established technique (Clarke et al., 2007; Correa et al., 2007; Domon et al., 2011; Ersek et al.,
377 2015; Ilangumaran et al., 1996; Liu et al., 2013; Liu et al., 2015; Mazzone et al., 2006; Nguyen et

al., 2007; Pang et al., 2004; Pristera et al., 2012; Russelakis-Carneiro et al., 2004; Tauzin et al., 2008; Waugh, 2013; Waugh et al., 2011a; Waugh et al., 2011b) to generate a composite yet simple signal to assess if there was any redistribution of these structurally related non-sterol molecules in the density gradient following cyclodextrin addition (figure 4). We observed that the ganglioside content of the buoyant fractions was decreased by about 50% following cyclodextrin treatment and this is consistent with mathematical analysis that vesicle size reduction is due to the non-selective desorption of membrane lipids.

386 **Discussion**

387 Our combined biophysical, biochemical, and mathematical analyses demonstrate that
388 cyclodextrin-induced cholesterol extraction can lead to an increase in equilibrium density by
389 inducing membrane shrinkage. The cyclodextrin-induced shift of biomolecules to a denser
390 membrane fraction can be accounted for by a large change in vesicle volume, without
391 necessarily having to evoke the disruption of liquid-ordered membrane microdomains. These
392 new findings have implications for the use of cyclodextrin-induced sterol depletion as a means
393 of assessing whether a protein associates with cholesterol-rich lipid rafts. At high cholesterol
394 levels, such as those reported here in the control buoyant membranes, one might expect
395 significant levels of lipid rafts or even for the entire membrane to exist solely in the liquid-
396 ordered phase (Almeida et al., 2005; Armstrong et al., 2013; Munro, 2003; Swamy et al., 2006)
397 and hence, removal of cholesterol with cyclodextrin would be predicted to disrupt these rafts
398 (Cabrera-Poch et al., 2004; Kabouridis et al., 2000; Larbi et al., 2004). However, in the context of
399 the type of experiments described here, a cyclodextrin-dependent change in membrane density
400 may only imply that a biomolecule is associated with a cholesterol-rich membrane and does not
401 necessarily report the stable association of that component with lipid raft microdomains.

402 Our results suggest that at least under the experimental conditions employed here,
403 cyclodextrin-induced reduction of membrane size can also be effected by the extraction of
404 molecules other than sterols. The apparent lack of selectivity for cyclodextrin-induced
405 biomolecule desorption demonstrated here leads us to speculate that these agents could
406 potentially be repurposed to treat a range of conditions similar to Niemann-Pick type C, that
407 feature enlarged endosomal membrane phenotypes due to defective lipid trafficking and/or
408 metabolism but importantly, do not necessarily involve cholesterol accumulation. An example

409 of a disease to consider in this regard could be oculocerebrorenal syndrome of Lowe (OCRL), a
410 neurodevelopmental condition characterized by phosphatidylinositol 4,5-bisphosphate
411 accumulation on endosomal membranes due to inactivating mutations in the OCRL
412 phosphoinositide 5-phosphatase (reviewed in (Billcliff and Lowe, 2014; Clayton et al., 2013b)).
413 Furthermore, whilst cyclodextrin has a high affinity for sterol lipids it is also known to bind
414 phosphoinositides such as phosphatidylinositol 4-phosphate (Davis et al., 2004), and this
415 further supports the idea that these macromolecules could have applications in the treatment
416 of a number of inherited phospholipid storage disorders. This suggests a new type of drug
417 action involving agents designed to alter membrane surface area through the reduction of
418 membrane mass. The objective of such treatments would be to increase the membrane
419 concentrations of more cyclodextrin-resistant biomolecules, in order to restore or amplify
420 membrane-based signaling or trafficking functions. This has already been shown for the
421 epidermal growth factor receptor, which is subject to augmented levels of constitutive
422 activation following cyclodextrin treatment (Pike and Casey, 2002; Westover et al., 2003).
423 However, these possible uses for cyclodextrin remain speculative and further work is required
424 to investigate if the biophysical changes documented here under specific in vitro conditions also
425 occur on intracellular membranes in live cells.

426 In conclusion, this work throws new light on the mechanism of action of methyl-β-cyclodextrin
427 on biological membranes. This may lead to a reassessment of its use in cell-based laboratory
428 experiments while at the same time widening its potential applications in the therapeutic arena.
429 In particular, this study indicates that the cholesterol-independent effects of cyclodextrin on
430 membrane area may have more general applications in the treatment of intracellular lipid
431 storage diseases.

432

References

Almeida, P.F., Pokorny, A., and Hinderliter, A. (2005). Thermodynamics of membrane domains. Biochim Biophys Acta *1720*, 1-13.

Armstrong, C.L., Marquardt, D., Dies, H., Kucerka, N., Yamani, Z., Harroun, T.A., Katsaras, J., Shi, A.C., and Rheinstadter, M.C. (2013). The Observation of Highly Ordered Domains in Membranes with Cholesterol. PLoS One *8*, e66162.

Barylko, B., Mao, Y.S., Wlodarski, P., Jung, G., Binns, D.D., Sun, H.Q., Yin, H.L., and Albanesi, J.P. (2009). Palmitoylation controls the catalytic activity and subcellular distribution of phosphatidylinositol 4-kinase II{alpha}. J Biol Chem *284*, 9994-10003.

Bate, C., Tayebi, M., and Williams, A. (2008). Sequestration of free cholesterol in cell membranes by prions correlates with cytoplasmic phospholipase A2 activation. BMC Biol *6*, 8.

Billcliff, P.G., and Lowe, M. (2014). Inositol lipid phosphatases in membrane trafficking and human disease. Biochem J *461*, 159-175.

Cabrera-Poch, N., Sanchez-Ruiloba, L., Rodriguez-Martinez, M., and Iglesias, T. (2004). Lipid raft disruption triggers protein kinase C and Src-dependent protein kinase D activation and Kidins220 phosphorylation in neuronal cells. J Biol Chem *279*, 28592-28602.

Camargo, F., Erickson, R.P., Garver, W.S., Hossain, G.S., Carbone, P.N., Heidenreich, R.A., and Blanchard, J. (2001). Cyclodextrins in the treatment of a mouse model of Niemann-Pick C disease. Life Sci *70*, 131-142.

Chick, H., and Martin, C.J. (1913). The Density and Solution Volume of some Proteins. Biochem J *7*, 92-96.

Chu, K.M., Minogue, S., Hsuan, J.J., and Waugh, M.G. (2010). Differential effects of the phosphatidylinositol 4-kinases, PI4KIIalpha and PI4KIIIbeta, on Akt activation and apoptosis. Cell Death Dis *1*, e106.

Clarke, C.J., Ohanian, V., and Ohanian, J. (2007). Norepinephrine and endothelin activate diacylglycerol kinases in caveolae/rafts of rat mesenteric arteries: agonist-specific role of PI3-kinase. American journal of physiology. Heart and circulatory physiology *292*, H2248-2256.

Clayton, E.L., Minogue, S., and Waugh, M.G. (2013a). Mammalian phosphatidylinositol 4-kinases as modulators of membrane trafficking and lipid signaling networks. Prog Lipid Res *52*, 294-304.

Clayton, E.L., Minogue, S., and Waugh, M.G. (2013b). Phosphatidylinositol 4-kinases and PI4P metabolism in the nervous system: roles in psychiatric and neurological diseases. Mol Neurobiol *47*, 361-372.

Correa, J.R., Atella, G.C., Vargas, C., and Soares, M.J. (2007). Transferrin uptake may occur through detergent-resistant membrane domains at the cytopharynx of Trypanosoma cruzi epimastigote forms. Mem Inst Oswaldo Cruz *102*, 871-876.

Davidson, C.D., Ali, N.F., Micsenyi, M.C., Stephney, G., Renault, S., Dobrenis, K., Ory, D.S., Vanier, M.T., and Walkley, S.U. (2009). Chronic cyclodextrin treatment of murine Niemann-Pick C disease ameliorates neuronal cholesterol and glycosphingolipid storage and disease progression. PLoS One *4*, e6951.

Davis, A.J., Perera, I.Y., and Boss, W.F. (2004). Cyclodextrins enhance recombinant phosphatidylinositol phosphate kinase activity. J Lipid Res *45*, 1783-1789.

Dawson, R.M.C., Elliot, D.C., Elliot, W.H., and Jones, K.M. (1986). Data for Biochemical Research, Third edn (Oxford Science Publications).

Domon, M.M., Besson, F., Bandorowicz-Pikula, J., and Pikula, S. (2011). Annexin A6 is recruited into lipid rafts of Niemann-Pick type C disease fibroblasts in a Ca2+-dependent manner. Biochem Biophys Res Commun *405*, 192-196.

Ersek, A., Xu, K., Antonopoulos, A., Butters, T.D., Santo, A.E., Vattakuzhi, Y., Williams, L.M., Goudevenou, K., Danks, L., Freidin, A*., et al.* (2015). Glycosphingolipid synthesis inhibition limits osteoclast activation and myeloma bone disease. J Clin Invest *125*, 2279-2292.

Fischer, H., Polikarpov, I., and Craievich, A.F. (2004). Average protein density is a molecular-weight-dependent function. Protein Sci *13*, 2825-2828.

Ford, C.P., Stemkowski, P.L., Light, P.E., and Smith, P.A. (2003). Experiments to test the role of phosphatidylinositol 4,5-bisphosphate in neurotransmitter-induced M-channel closure in bullfrog sympathetic neurons. J Neurosci *23*, 4931-4941.

Fujiki, Y., Hubbard, A.L., Fowler, S., and Lazarow, P.B. (1982). Isolation of intracellular membranes by means of sodium carbonate treatment: application to endoplasmic reticulum. J Cell Biol *93*, 97-102.

Haynes, W.M. (2005). CRC Handbook of Chemistry and Physics, 94 edn (Taylor & Francis Group).

Heine, T., Dos Santos, H.F., Patchkovskii, S., and Duarte, H.A. (2007). Structure and dynamics of beta-cyclodextrin in aqueous solution at the density-functional tight binding level. J Phys Chem A *111*, 5648-5654.

Hill, W.G., An, B., and Johnson, J.P. (2002). Endogenously expressed epithelial sodium channel is present in lipid rafts in A6 cells. J Biol Chem *277*, 33541-33544.

Holtta-Vuori, M., Tanhuanpaa, K., Mobius, W., Somerharju, P., and Ikonen, E. (2002). Modulation of cellular cholesterol transport and homeostasis by Rab11. Mol Biol Cell *13*, 3107-3122.

Ilangumaran, S., Arni, S., Chicheportiche, Y., Briol, A., and Hoessli, D.C. (1996). Evaluation by dot-immunoassay of the differential distribution of cell surface and intracellular proteins in glycosylphosphatidylinositol-rich plasma membrane domains. Anal Biochem *235*, 49-56.

Kabouridis, P.S., Janzen, J., Magee, A.L., and Ley, S.C. (2000). Cholesterol depletion disrupts lipid rafts and modulates the activity of multiple signaling pathways in T lymphocytes. Eur J Immunol *30*, 954-963.

Kuziemko, G.M., Stroh, M., and Stevens, R.C. (1996). Cholera toxin binding affinity and specificity for gangliosides determined by surface plasmon resonance. Biochemistry *35*, 6375-6384.

Larbi, A., Douziech, N., Khalil, A., Dupuis, G., Gherairi, S., Guerard, K.P., and Fulop, T., Jr. (2004). Effects of methyl-beta-cyclodextrin on T lymphocytes lipid rafts with aging. Exp Gerontol *39*, 551-558.

Li, J., Lu, Y., Zhang, J., Kang, H., Qin, Z., and Chen, C. (2010). PI4KIIalpha is a novel regulator of tumor growth by its action on angiogenesis and HIF-1alpha regulation. Oncogene *29*, 2550-2559.

Li, J., Zhang, L., Gao, Z., Kang, H., Rong, G., Zhang, X., and Chen, C. (2014). Dual inhibition of EGFR at protein and activity level via combinatorial blocking of PI4KIIalpha as anti-tumor strategy. Protein Cell *5*, 457-468.

Lim, C.H., Schoonderwoerd, K., Kleijer, W.J., de Jonge, H.R., and Tilly, B.C. (2006). Regulation of the cell swelling-activated chloride conductance by cholesterol-rich membrane domains. Acta Physiol (Oxf) *187*, 295-303.

Liu, B., Li, H., Repa, J.J., Turley, S.D., and Dietschy, J.M. (2008). Genetic variations and treatments that affect the lifespan of the NPC1 mouse. J Lipid Res *49*, 663-669.

Liu, B., Ramirez, C.M., Miller, A.M., Repa, J.J., Turley, S.D., and Dietschy, J.M. (2010). Cyclodextrin overcomes the transport defect in nearly every organ of NPC1 mice leading to excretion of sequestered cholesterol as bile acid. J Lipid Res *51*, 933-944.

Liu, B., Turley, S.D., Burns, D.K., Miller, A.M., Repa, J.J., and Dietschy, J.M. (2009). Reversal of defective lysosomal transport in NPC disease ameliorates liver dysfunction and neurodegeneration in the npc1-/- mouse. Proc Natl Acad Sci U S A *106*, 2377-2382.

Liu, Q., Yao, W.D., and Suzuki, T. (2013). Specific interaction of postsynaptic densities with membrane rafts isolated from synaptic plasma membranes. J Neurogenet *27*, 43-58.

Liu, T.M., Ling, Y., Woyach, J.A., Beckwith, K., Yeh, Y.Y., Hertlein, E., Zhang, X., Lehman, A., Awan, F., Jones, J.A*., et al.* (2015). OSU-T315: a novel targeted therapeutic that antagonizes AKT membrane localization and activation of chronic lymphocytic leukemia cells. Blood *125*, 284-295.

Loftsson, T., and Brewster, M.E. (1996). Pharmaceutical applications of cyclodextrins. 1. Drug solubilization and stabilization. J Pharm Sci *85*, 1017-1025.

Lu, D., Sun, H.Q., Wang, H., Barylko, B., Fukata, Y., Fukata, M., Albanesi, J.P., and Yin, H.L. (2012). Phosphatidylinositol 4-kinase IIalpha is palmitoylated by Golgi-localized palmitoyltransferases in cholesterol-dependent manner. J Biol Chem *287*, 21856-21865.

Matarazzo, S., Quitadamo, M.C., Mango, R., Ciccone, S., Novelli, G., and Biocca, S. (2012). Cholesterol-lowering drugs inhibit lectin-like oxidized low-density lipoprotein-1 receptor function by membrane raft disruption. Mol Pharmacol *82*, 246-254.

Mazzone, A., Tietz, P., Jefferson, J., Pagano, R., and LaRusso, N.F. (2006). Isolation and characterization of lipid microdomains from apical and basolateral plasma membranes of rat hepatocytes. Hepatology *43*, 287-296.

Mbua, N.E., Flanagan-Steet, H., Johnson, S., Wolfert, M.A., Boons, G.J., and Steet, R. (2013). Abnormal accumulation and recycling of glycoproteins visualized in Niemann-Pick type C cells using the chemical reporter strategy. Proc Natl Acad Sci U S A *110*, 10207-10212.

Minogue, S., Chu, K.M., Westover, E.J., Covey, D.F., Hsuan, J.J., and Waugh, M.G. (2010). Relationship between phosphatidylinositol 4-phosphate synthesis, membrane organization, and lateral diffusion of PI4KIIalpha at the trans-Golgi network. J Lipid Res *51*, 2314-2324.

Munro, S. (2003). Lipid rafts: elusive or illusive? Cell *115*, 377-388.

Navratil, A.M., Bliss, S.P., Berghorn, K.A., Haughian, J.M., Farmerie, T.A., Graham, J.K., Clay, C.M., and Roberson, M.S. (2003). Constitutive localization of the gonadotropin-releasing hormone (GnRH) receptor to low density membrane microdomains is necessary for GnRH signaling to ERK. J Biol Chem *278*, 31593-31602.

Nebl, T., Pestonjamasp, K.N., Leszyk, J.D., Crowley, J.L., Oh, S.W., and Luna, E.J. (2002). Proteomic analysis of a detergent-resistant membrane skeleton from neutrophil plasma membranes. J Biol Chem *277*, 43399-43409.

Nguyen, H.T., Charrier-Hisamuddin, L., Dalmasso, G., Hiol, A., Sitaraman, S., and Merlin, D. (2007). Association of PepT1 with lipid rafts differently modulates its transport activity in polarized and nonpolarized cells. American journal of physiology. Gastrointestinal and liver physiology *293*, G1155-1165.

Nicholson, A.M., and Ferreira, A. (2009). Increased membrane cholesterol might render mature hippocampal neurons more susceptible to beta-amyloid-induced calpain activation and tau toxicity. J Neurosci *29*, 4640-4651.

Ottico, E., Prinetti, A., Prioni, S., Giannotta, C., Basso, L., Chigorno, V., and Sonnino, S. (2003). Dynamics of membrane lipid domains in neuronal cells differentiated in culture. J Lipid Res *44*, 2142-2151.

Paladino, S., Lebreton, S., Tivodar, S., Formiggini, F., Ossato, G., Gratton, E., Tramier, M., Coppey-Moisan, M., and Zurzolo, C. (2014). Golgi sorting regulates organization and activity of GPI proteins at apical membranes. Nat Chem Biol *10*, 350-357.

Pang, S., Urquhart, P., and Hooper, N.M. (2004). N-glycans, not the GPI anchor, mediate the apical targeting of a naturally glycosylated, GPI-anchored protein in polarised epithelial cells. J Cell Sci *117*, 5079-5086.

Pike, L.J., and Casey, L. (2002). Cholesterol levels modulate EGF receptor-mediated signaling by altering receptor function and trafficking. Biochemistry *41*, 10315-10322.

Pike, L.J., and Miller, J.M. (1998). Cholesterol depletion delocalizes phosphatidylinositol bisphosphate and inhibits hormone-stimulated phosphatidylinositol turnover. J Biol Chem *273*, 22298-22304.

Pinjari, R.V., Joshi, K.A., and Gejji, S.P. (2006). Molecular electrostatic potentials and hydrogen bonding in alpha-, beta-, and gamma-cyclodextrins. J Phys Chem A *110*, 13073-13080.

573 Pontikis, C.C., Davidson, C.D., Walkley, S.U., Platt, F.M., and Begley, D.J. (2013). Cyclodextrin alleviates
574 neuronal storage of cholesterol in Niemann-Pick C disease without evidence of detectable blood-brain
575 barrier permeability. J Inherit Metab Dis *36*, 491-498.
576 Pristera, A., Baker, M.D., and Okuse, K. (2012). Association between tetrodotoxin resistant channels and
577 lipid rafts regulates sensory neuron excitability. PLoS One *7*, e40079.
578 Ramirez, C.M., Liu, B., Aqul, A., Taylor, A.M., Repa, J.J., Turley, S.D., and Dietschy, J.M. Quantitative role
579 of LAL, NPC2, and NPC1 in lysosomal cholesterol processing defined by genetic and pharmacological
580 manipulations. J Lipid Res *52*, 688-698.
581 Ramirez, C.M., Liu, B., Taylor, A.M., Repa, J.J., Burns, D.K., Weinberg, A.G., Turley, S.D., and Dietschy,
582 J.M. (2010). Weekly cyclodextrin administration normalizes cholesterol metabolism in nearly every
583 organ of the Niemann-Pick type C1 mouse and markedly prolongs life. Pediatr Res *68*, 309-315.
584 Rodal, S.K., Skretting, G., Garred, O., Vilhardt, F., van Deurs, B., and Sandvig, K. (1999). Extraction of
585 cholesterol with methyl-beta-cyclodextrin perturbs formation of clathrin-coated endocytic vesicles. Mol
586 Biol Cell *10*, 961-974.
587 Rosenbaum, A.I., Zhang, G., Warren, J.D., and Maxfield, F.R. (2010). Endocytosis of beta-cyclodextrins is
588 responsible for cholesterol reduction in Niemann-Pick type C mutant cells. Proc Natl Acad Sci U S A *107*,
589 5477-5482.
590 Russelakis-Carneiro, M., Hetz, C., Maundrell, K., and Soto, C. (2004). Prion replication alters the
591 distribution of synaptophysin and caveolin 1 in neuronal lipid rafts. Am J Pathol *165*, 1839-1848.
592 Shogomori, H., and Futerman, A.H. (2001). Cholesterol depletion by methyl-beta-cyclodextrin blocks
593 cholera toxin transport from endosomes to the Golgi apparatus in hippocampal neurons. J Neurochem
594 *78*, 991-999.
595 Simons, J.P., Al-Shawi, R., Minogue, S., Waugh, M.G., Wiedemann, C., Evangelou, S., Loesch, A., Sihra,
596 T.S., King, R., Warner, T.T.*, et al.* (2009). Loss of phosphatidylinositol 4-kinase 2alpha activity causes late
597 onset degeneration of spinal cord axons. Proc Natl Acad Sci U S A *106*, 11535-11539.
598 Spisni, E., Griffoni, C., Santi, S., Riccio, M., Marulli, R., Bartolini, G., Toni, M., Ullrich, V., and Tomasi, V.
599 (2001). Colocalization prostacyclin (PGI2) synthase--caveolin-1 in endothelial cells and new roles for PGI2
600 in angiogenesis. Exp Cell Res *266*, 31-43.
601 Swamy, M.J., Ciani, L., Ge, M., Smith, A.K., Holowka, D., Baird, B., and Freed, J.H. (2006). Coexisting
602 domains in the plasma membranes of live cells characterized by spin-label ESR spectroscopy. Biophys J
603 *90*, 4452-4465.
604 Swaroop, M., Thorne, N., Rao, M.S., Austin, C.P., McKew, J.C., and Zheng, W. (2012). Evaluation of
605 cholesterol reduction activity of methyl-beta-cyclodextrin using differentiated human neurons and
606 astrocytes. Journal of biomolecular screening *17*, 1243-1251.

607 Tauzin, S., Ding, H., Khatib, K., Ahmad, I., Burdevet, D., van Echten-Deckert, G., Lindquist, J.A., Schraven,
608 B., Din, N.U., Borisch, B*., et al.* (2008). Oncogenic association of the Cbp/PAG adaptor protein with the
609 Lyn tyrosine kinase in human B-NHL rafts. Blood *111*, 2310-2320.
610 te Vruchte, D., Speak, A.O., Wallom, K.L., Al Eisa, N., Smith, D.A., Hendriksz, C.J., Simmons, L., Lachmann,
611 R.H., Cousins, A., Hartung, R*., et al.* (2014). Relative acidic compartment volume as a lysosomal storage
612 disorder-associated biomarker. J Clin Invest *124*, 1320-1328.
613 Vance, J.E., and Karten, B. (2014). Niemann-Pick C disease and mobilization of lysosomal cholesterol by
614 cyclodextrin. J Lipid Res *55*, 1609-1621.
615 Vite, C.H., Bagel, J.H., Swain, G.P., Prociuk, M., Sikora, T.U., Stein, V.M., O'Donnell, P., Ruane, T., Ward,
616 S., Crooks, A*., et al.* (2015). Intracisternal cyclodextrin prevents cerebellar dysfunction and Purkinje cell
617 death in feline Niemann-Pick type C1 disease. Sci Transl Med *7*, 276ra226.
618 Waugh, M.G. (2012). Phosphatidylinositol 4-kinases, phosphatidylinositol 4-phosphate and cancer.
619 Cancer Lett *325*, 125-131.
620 Waugh, M.G. (2013). Raft-like membranes from the trans-Golgi network and endosomal compartments.
621 Nat Protoc *8*, 2429-2439.
622 Waugh, M.G. (2014). Chromosomal Instability and Phosphoinositide Pathway Gene Signatures in
623 Glioblastoma Multiforme. Mol Neurobiol.
624 Waugh, M.G. (2015). PIPs in neurological diseases. Biochim Biophys Acta *1851*, 1066-1082.
625 Waugh, M.G., Chu, K.M., Clayton, E.L., Minogue, S., and Hsuan, J.J. (2011a). Detergent-free isolation and
626 characterization of cholesterol-rich membrane domains from trans-Golgi network vesicles. J Lipid Res
627 *52*, 582-589.
628 Waugh, M.G., Lawson, D., and Hsuan, J.J. (1999). Epidermal growth factor receptor activation is localized
629 within low-buoyant density, non-caveolar membrane domains. Biochem J *337 (Pt 3)*, 591-597.
630 Waugh, M.G., Lawson, D., Tan, S.K., and Hsuan, J.J. (1998). Phosphatidylinositol 4-phosphate synthesis in
631 immunoisolated caveolae-like vesicles and low buoyant density non-caveolar membranes. J Biol Chem
632 *273*, 17115-17121.
633 Waugh, M.G., Minogue, S., Anderson, J.S., Balinger, A., Blumenkrantz, D., Calnan, D.P., Cramer, R., and
634 Hsuan, J.J. (2003a). Localization of a highly active pool of type II phosphatidylinositol 4-kinase in a
635 p97/valosin-containing-protein-rich fraction of the endoplasmic reticulum. Biochem J *373*, 57-63.
636 Waugh, M.G., Minogue, S., Blumenkrantz, D., Anderson, J.S., and Hsuan, J.J. (2003b). Identification and
637 characterization of differentially active pools of type IIalpha phosphatidylinositol 4-kinase activity in
638 unstimulated A431 cells. Biochem J *376*, 497-503.
639 Waugh, M.G., Minogue, S., Chotai, D., Berditchevski, F., and Hsuan, J.J. (2006). Lipid and peptide control
640 of phosphatidylinositol 4-kinase IIalpha activity on Golgi-endosomal rafts. J Biol Chem *281*, 3757-3763.

641 Waugh, M.G., Minogue, S., Clayton, E.L., and Hsuan, J.J. (2011b). CDP-diacylglycerol phospholipid
642 synthesis in detergent-soluble, non-raft, membrane microdomains of the endoplasmic reticulum. J Lipid
643 Res *52*, 2148-2158.
644 Welliver, M. (2006). New drug sugammadex: a selective relaxant binding agent. AANA J *74*, 357-363.
645 Westover, E.J., Covey, D.F., Brockman, H.L., Brown, R.E., and Pike, L.J. (2003). Cholesterol depletion
646 results in site-specific increases in epidermal growth factor receptor phosphorylation due to membrane
647 level effects. Studies with cholesterol enantiomers. J Biol Chem *278*, 51125-51133.
648 Xu, W., Yoon, S.I., Huang, P., Wang, Y., Chen, C., Chong, P.L., and Liu-Chen, L.Y. (2006). Localization of
649 the kappa opioid receptor in lipid rafts. J Pharmacol Exp Ther *317*, 1295-1306.
650 Zidovetzki, R., and Levitan, I. (2007). Use of cyclodextrins to manipulate plasma membrane cholesterol
651 content: evidence, misconceptions and control strategies. Biochim Biophys Acta *1768*, 1311-1324.

652

653

654 **Legends**

655

656 **Figure 1.**

657 Flow chart outlining the steps involved in the subcellular fractionation procedures, equilibrium
658 density floatation assay and membrane analyses used in the experiments.

659

660 **Figure 2.**

661 Comparing the effects of cyclodextrin treatment on the biochemical composition of buoyant
662 and dense membrane fractions isolated on equilibrium sucrose density gradients. (A) Change in
663 cholesterol levels as determined by Amplex Red cholesterol assays. Note that there was no
664 significant change in the total amount of cholesterol present in the dense membranes. (B)
665 Levels of the membrane-associated protein PI4KIIα were determined by Western blotting and
666 quantitated by image analysis software. Cyclodextrin addition causes a redistribution of PI4KIIα
667 from the buoyant to the dense fractions. Results are presented as mean ± S.E.M from
668 experiments repeated three times, *** $p < 0.001$, ** $p < 0.01$, NS not statistically significant
669 using the two-tailed student t-test.

670

671 **Figure 3.**

672 The density of each gradient fraction was determined by refractometry and the conversion of
673 refractive index values to sucrose concentrations was accomplished using Blix tables. Results
674 are presented as mean ± S.E.M of an experiment repeated three times.

675

676 **Figure 4**

677 Dot blotting of equal volume membrane fractions and detection with HRP-conjugated cholera
678 toxin B subunit was used to determine the levels of ganglioside lipids in control and
679 cyclodextrin-treated membrane fractions. Cyclodextrin addition resulted in a decrease in HRP-
680 conjugated cholera toxin B subunit binding to the buoyant membrane fractions. Results are
681 presented as mean ± S.E.M from experiments repeated three times.
682

683 **Table 1.**

684 The size distributions, as measured by dynamic light scattering, of control and cyclodextrin-
685 treated membrane vesicles from different gradient fractions. Results are presented as the mean
686 ± S.D. of triplicate determinations.
687

688

689

690

691 Table 1. Size of membrane vesicles in different gradient fractions following cholesterol

692 depletion with cyclodextrin.

693

Treatment	Gradient Fraction	Size (nm)
Control	Buoyant	779.5 ± 28.2
	Dense	453.0 ± 177.1
Cholesterol Depletion	Buoyant	42.2 ± 11.5
	Dense	270.2 ± 68.8

694

695

696

697

698

699

700

Figure 1(on next page)

Flow chart of steps involved in the subcellular fractionation procedures

Figure 1: Flow chart outlining the steps involved in the subcellular fractionation procedures, equilibrium density floatation assay and membrane analyses used in the experiments.

Figure 1

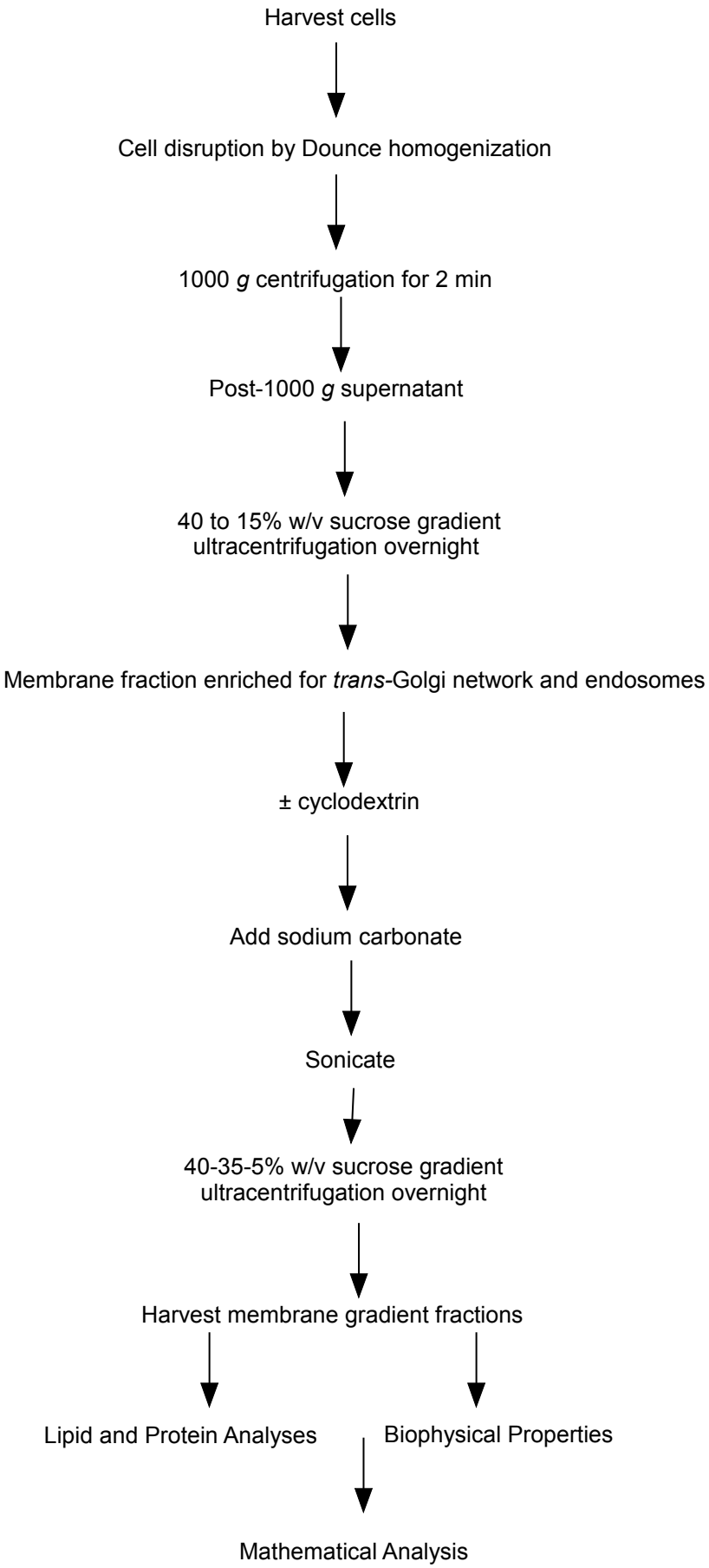
Harvest cells
Cell disruption by Dounce homogenization
1000 *g* centrifugation for 2 min
Post-1000 *g* supernatant
40 to 15% w/v sucrose gradient ultracentrifugation overnight
Membrane fraction enriched for *trans*-Golgi network and endosomes
± cyclodextrin
Add sodium carbonate
Sonicate
40-35-5% w/v sucrose gradient ultracentrifugation overnight
Harvest membrane gradient fractions
Lipid and Protein Analyses
Biophysical Properties
Mathematical Analysis

2

Effects of cyclodextrin on vesicle composition

Figure 2: Comparing the effects of cyclodextrin treatment on the biochemical composition of buoyant and dense membrane fractions isolated on equilibrium sucrose density gradients. (A) Change in cholesterol levels as determined by Amplex Red cholesterol assays. Note that there was no significant change in the total amount of cholesterol present in the dense membranes. (B) Levels of the membrane - associated protein PI4KIIalpha were determined by Western blotting and quantitated by image analysis software. Cyclodextrin addition causes a redistribution of PI4KIIalpha from the buoyant to the dense fractions. Results are presented as mean ± S.E.M from experiments repeated three times, *** $p < 0.001$, ** $p < 0.01$, NS not statistically significant using the two-tailed student t-test.

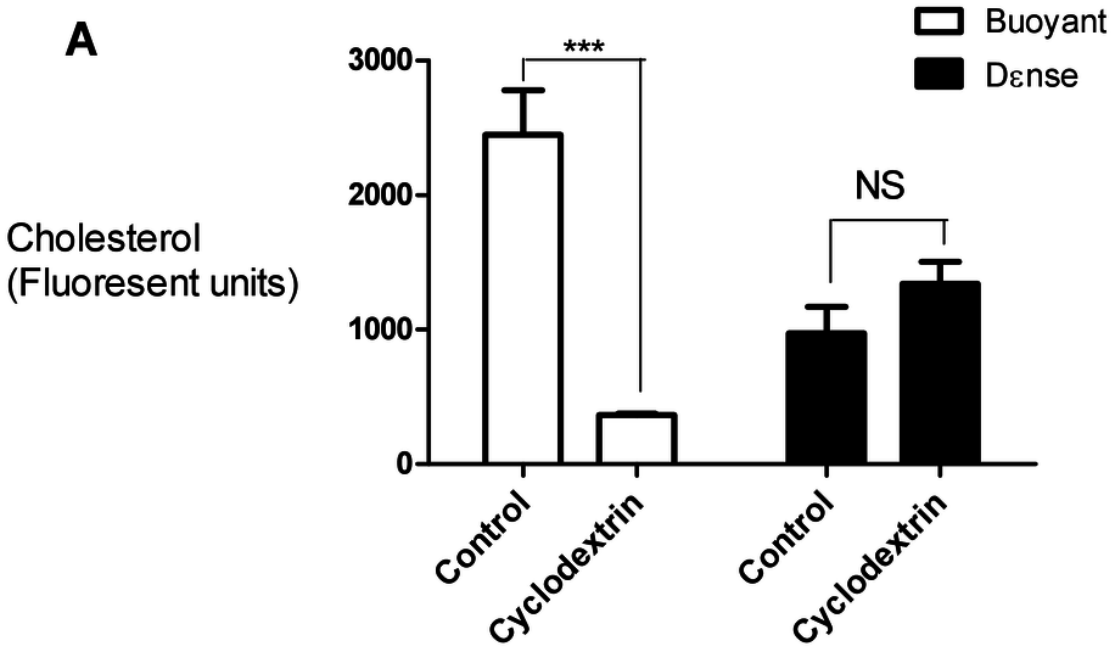
A
Buoyant
Dεnse
***
NS
3000
2000
1000
0
Cholesterol
(Fluoresent units)
Control
Cyclodextrin
Control
Cyclodextrin

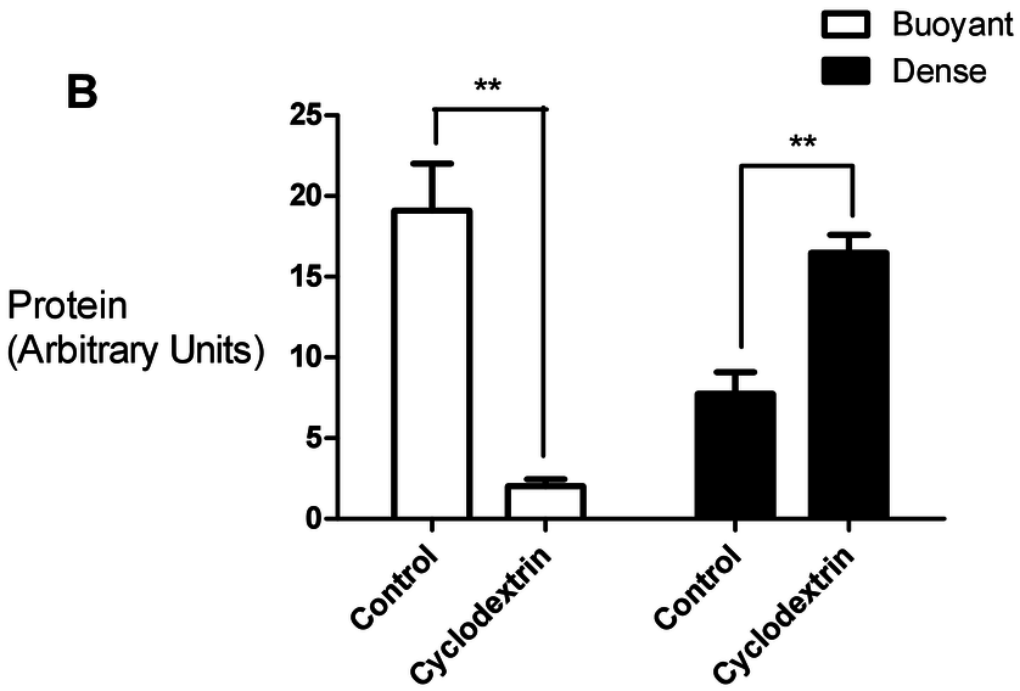
B
Buoyant
Dense
**
**
25
20
15
10
5
0
Protein
(Arbitrary Units)
Control
Cyclodextrin
Control
Cyclodextrin

3

Sucrose density gradient profile

Figure 3: The density of each gradient fraction was determined by refractometry and the conversion of refractive index values to sucrose concentrations was accomplished using Blix tables. Results are presented as mean ± S.E.M of an experiment repeated three times.

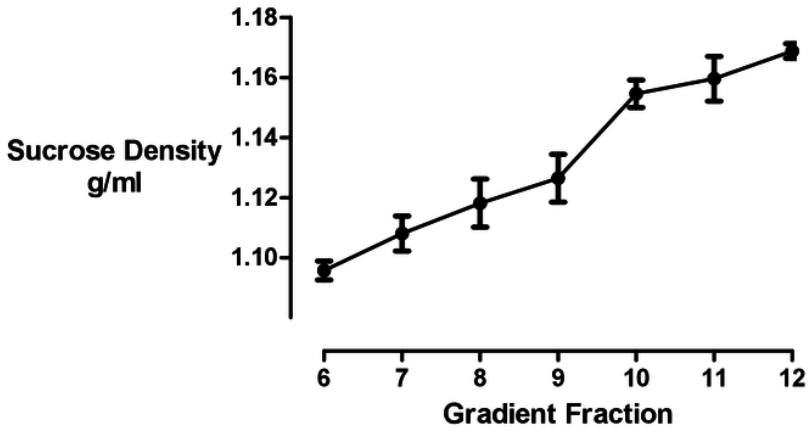
Sucrose Density
g/ml
1.18
1.16
1.14
1.12
1.10
6
7
8
9
10
11
12
Gradient Fraction

4

Effect of cyclodextrin on ganglioside distribution profile

Figure 4: Dot blotting of equal volume membrane fractions and detection with HRP-conjugated cholera toxin B subunit was used to determine the levels of ganglioside lipids in control and cyclodextrin-treated membrane fractions. Cyclodextrin addition resulted in a decrease in HRP-conjugated cholera toxin B subunit binding to the buoyant membrane fractions. Results are presented as mean ± S.E.M from experiments repeated three times.

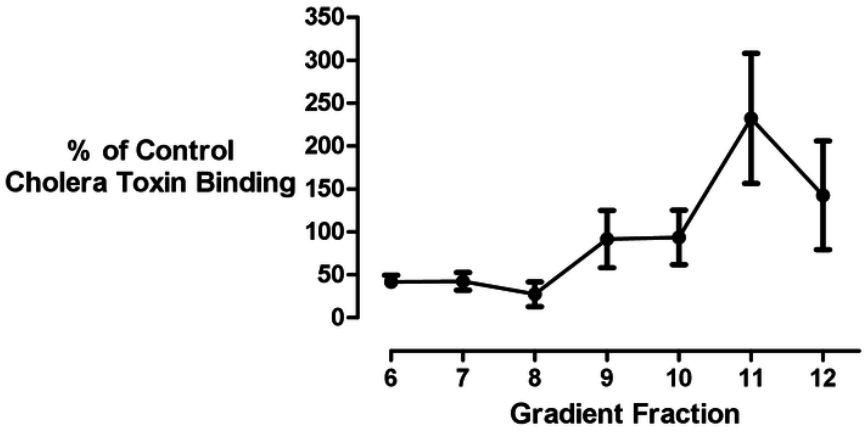
% of Control
Cholera Toxin Binding
350
300
250
200
150
100
50
0
6
7
8
9
10
11
12
Gradient Fraction

Table 1(on next page)

Size ofmembrane vesicles in different gradient fraction s following cholesterol depletion with cyclodextrin.

Table 1: The size distributions, as measured by dynamic light scattering, of control and cyclodextrin-treated membrane vesicles from different gradient fractions. Results are presented as the mean ± S.D. of triplicate determinations.

1

Treatment	Gradient Fraction	Size (nm)
Control	Buoyant	779.5 ± 28.2
	Dense	453.0 ± 177.1
Cholesterol Depletion	Buoyant	42.2 ± 11.5
	Dense	270.2 ± 68.8

2